International Journal of Modern Physics B
(2025) 2550239 (10 pages)

DOI: 10.1142/S021797922550239X

The crystal and magnetic structure of the cation-disordered perovskites $LaCo_{0.5}Mn_{0.5}O_3$ and $YCo_{0.5}Mn_{0.5}O_3$

L. H. Khiem [*,†], S. E. Kichanov [‡], O. N. Lis [‡], N. T. Nguyen [‡,§,¶,††], E. V. Lukin [‡], T. N. Vershinina [‡], D. P. Kozlenko [‡], N. O. Golosova [‡], N. Truong-Tho [§], N. T. Dang [‖,**] and T. P. Hoang [‖,**]

[*]*Institute of Physics, Vietnam Academy of Science and Technology, Hanoi 100000, Vietnam*

[†]*Graduate University of Science and Technology, Vietnam Academy of Science and Technology, Hanoi 100000, Vietnam*

[‡]*Frank Laboratory of Neutron Physics, Joint Institute for Nuclear Research, Dubna 141980, Russia*

[§]*Faculty of Electronics, Electrical Engineering and Material Technology, University of Sciences, Hue University, Hue 530000, Vietnam*

[¶]*Institute of Oceanography, Vietnam Academy of Science and Technology, Nha Trang 650000, Vietnam*

[‖]*Institute of Research and Development, Duy Tan University, Danang 550000, Vietnam*

[**]*Faculty of Environmental and Natural Sciences, Duy Tan University, Danang 550000, Vietnam*

[††]*ntnghiem1997@gmail.com*

Received 13 May 2025
Revised 2 July 2025
Accepted 17 July 2025
Published 30 August 2025

The crystal and magnetic structures of $LaCo_{0.5}Mn_{0.5}O_3$ and $YCo_{0.5}Mn_{0.5}O_3$ perovskites were studied using neutron and X-ray powder diffraction techniques in the temperature range of 15–300 K. The obtained structural data indicate a complete disorder of cobalt and manganese cations, resulting in an orthorhombic structure with the *Pnma* space group in both compounds. The temperature evolution of unit cell parameters, characteristic bond lengths and valence

[††] Corresponding author.

angles was studied for both compounds. Anomalies in the temperature behavior of the lattice parameters and oxygen octahedra distortions were observed. These anomalies are attributed to the formation of a ferromagnetic phase at $T_C = 76(1)$ K for $YCo_{0.5}Mn_{0.5}O_3$ and at $T_C = 218(1)$ K for $LaCo_{0.5}Mn_{0.5}O_3$.

Keywords: X-ray diffraction; neutron diffraction; crystal and magnetic structure; double perovskite oxides.

PACS numbers: 61.10.Nz, 61.12.Ld, 61.50.−f, 64.60.−i, 75.47.Lx

1. Introduction

Multiferroic materials exhibit strong coupling between electric and magnetic ordering, making them of both fundamental and technological interest.[1–3] The coexistence of polar phases and long-range magnetic order enables the development of innovative electronic devices that can manipulate magnetic properties via electric fields and *vice versa*. These multiferroic materials hold great promise for applications in memory and magnetic data storage devices,[4] as well as in the field of spintronics research.[5]

The advanced multiferroic materials are double perovskite oxides with the general formula of $A_2BB'O_6$, where A is an alkali metal or a rare earth ion and B or B′ are transition metals or lanthanide elements.[3,6,7] An ideal crystal lattice of ordered doubled perovskites can be seen as a symmetrical pattern of interlocked BO_6 and $B'O_6$ octahedral units that alternate in three directions within the crystal structure. Depending on the types of A, B and B′ cations, as well as the B/B′ ion radius ratios, the physical properties of these materials can vary greatly, including magnetoresistance, multiferroic phenomena, magnetic dielectric properties, and the magnetocaloric effect.[8,9] Recently, more and more attention has been paid to ordered double perovskites with rare earth ions in the A site and cobalt and manganese ions as B and B′ cations.[10,11] The different valences of manganese ions, variations in the spin states of cobalt ions and partial disordering of magnetic cations all contribute to the formation of puzzling magnetic properties in these types of double perovskite oxides.[11–13] Charge ordering, distortion of oxygen octahedral units, and topologically related magnetic frustration are the main causes of the multiferroic phenomenon in these compounds.[14]

In the ideal fully ordered structure of double perovskites, where the positions of Co^{2+} and Mn^{4+} ions are interchanged, a super-exchange magnetic interaction between cobalt and manganese ions leads to the formation of a long-range ferromagnetic (FM) order.[15,16] Interestingly, the Curie temperature depends strongly on the type of rare earth element. The cation disordering in the doubled perovskite can trigger an increase in Mn^{4+}–O–Mn^{4+} or Co^{2+}–O–Co^{2+} double exchange interactions that strengthen antiferromagnetic (AFM) couplings. Disorder of the Mn and Co cations between crystallographic sites leads to the emergence of non-collinear magnetic order or collinear antiferromagnetic ordering at low temperatures.[15,17,18]

In addition, structural distortions in MnO_6 and CoO_6 octahedral units cause weak magnetic interactions next-nearest-neighbor along the Mn–O–Co–O–Mn pathway, leading to magnetostrictive ferroelectricity due to cooperative displacement of rare earth and transition metal ions.[17]

Deviation from the ideal structural arrangement of Co^{2+} and Mn^{4+} cations, due to variations in synthesis approach, oxygen deficiency or doping of both the A sublattice and the B/B' sublattices, is one of the main factors contributing to the formation of the structural and magnetic properties in double perovskite materials.[17,19–21] As an example, structural disordering of cobalt and manganese ions in La_2CoMnO_6 compound leads to two ferromagnetic transitions, with Curie temperatures $T_{C1} \sim 220$ K for cation-ordered phase and an additional FM phase transition at temperatures below $T_{C2} \sim 150$ K related to cation-disorder structure.[15,17] The Coulomb-assisted spin-orbit coupling causes an insulating state in La_2CoMnO_6. On the other hand, the replacement of La^{3+} cations with other rare earth ions also leads to changes in the structural and physical properties. The changes in the lengths of the B–O and B′–O bonds and the angles between them affect the exchange interaction, significantly decreasing the Curie temperature. It has been reported that the FM state exists below $T_C \sim 75$ K for Y_2CoMnO_6 perovskite.[15,17] Both La_2CoMnO_6 and Y_2CoMnO_6 perovskite materials have a negative temperature coefficient of electrical resistance, indicating a semiconductor type of conductivity.[15]

A key factor in understanding the origin and changes in the physical properties of double perovskites is the degree of disorder of cations at different crystallographic sites.[17,22,23] Another important factor that seriously affects the magnetic and ferroelectric properties is the structural distortion of MnO_6 and CoO_6 polyhedra.[15] It is necessary to study these structural factors in detail. The neutron diffraction method is sensitive to the redistribution of cobalt and iron ions, which is very useful for further understanding the relationship between the structural and magnetic properties of this type of perovskite. Therefore, we have studied $YCo_{0.5}Mn_{0.5}O_3$ and $LaCo_{0.5}Mn_{0.5}O_3$ double perovskites using neutron diffraction in the temperature range of 5–300 K. We also studied the temperature evolution of crystal structure parameters in detail using complementary X-ray diffraction techniques.

2. Experimental

Polycrystalline samples of $YCo_{0.5}Mn_{0.5}O_3$ and $LaCo_{0.5}Mn_{0.5}O_3$ were synthesized using a conventional sol-gel method. High-purity yttrium nitrate hexahydrate ($Y(NO_3)_3 \cdot 6H_2O$) or lanthanum nitrate hexahydrate ($La(NO_3)_3 \cdot 6H_2O$), cobalt sulfate heptahydrate ($CoSO_4 \cdot 7H_2O$) and manganese nitrate tetrahydrate ($Mn(NO_3)_2 \cdot 4H_2O$) were used as starting materials. These precursors were mixed in stoichiometric ratios to form a homogeneous solution. Citric acid was added as a chelating agent, and the reaction was carried out in an alkaline medium. The solution was continuously stirred and gradually heated up to 450°C to facilitate gel formation

and subsequent decomposition. The resulting gel was ground into a fine powder and annealed at 1150°C for 12 h to yield the final product.

Neutron powder diffraction measurements were performed with the DN-12 diffractometer[24] at the IBR-2 high-flux pulsed reactor (FLNP, JINR, Dubna, Russia). Diffraction patterns were collected at scattering angles $2\theta = 90°$. The spectrometer resolution at $\lambda = 2$ Å was $\Delta d/d = 0.012$. Typical data collection time for a temperature point was 2 h. We studied samples with a volume of about 20 mm^3, placed inside a cryostat of the closed-cycle helium refrigerator, which cooled samples from room temperature down to 10 K.

The X-ray diffraction patterns were collected with the PANalytical Empyrean Advance X-ray diffractometer in Bragg–Brentano geometry with a Cu-K_α radiation source and the PIXcel 3D detector. The generator settings for the tube were 40 kV and 40 mA. Scanning was performed in the Bragg-Brentano geometry with a scattering angle 2θ in the range of $20° \leq 2\theta \leq 100°$ in 0.013° increments. The PANalytical Empyrean Advance X-ray diffractometer is equipped with an Oxford Cryosystem Phenix closed-cycle cryostat, which was used for low-temperature measurements in the range 15–300 K.

Neutron and X-ray diffraction data were analyzed using the Rietveld method with the FullProf software.[25]

3. Results

3.1. *X-ray diffraction*

The X-ray diffraction patterns of $YCo_{0.5}Mn_{0.5}O_3$ and $LaCo_{0.5}Mn_{0.5}O_3$ obtained at room temperature are shown in Fig. 1. Preliminary analysis of diffraction data

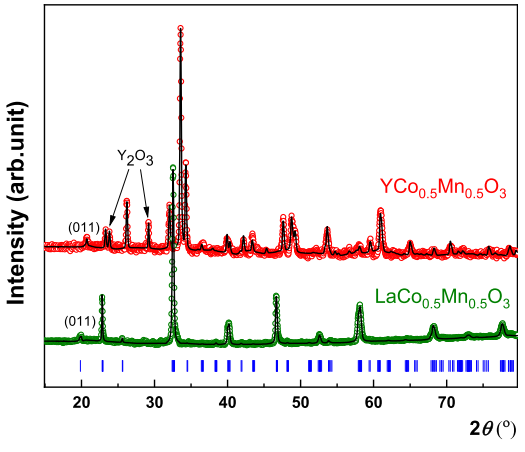

Fig. 1. (Color online) X-ray diffraction patterns of $YCo_{0.5}Mn_{0.5}O_3$ and $LaCo_{0.5}Mn_{0.5}O_3$ compounds were obtained under ambient conditions. The experimental data and the calculated profiles using the Rietveld method are presented. The vertical bars represent the calculated positions of diffraction peaks for the orthorhombic phase, while several peaks corresponding to an additional phase of Y_2O_3 are marked.

indicates that a monoclinic phase with the space group $P2_1/n$[14,15] did not provide a satisfactory fit to the experimental data using the Rietveld method. A comparative structural analysis of the monoclinic and orthorhombic models (see Supplementary Materials) showed that several characteristic reflections expected for the monoclinic phase were absent. The diffraction patterns could be successfully indexed using an orthorhombic unit cell with *Pnma* symmetry,[10] which directly indicates that both samples crystallize in a cation-distorted perovskite structure. In the orthorhombic phase, the lattice parameters correspond to the perovskite unit cell as $a \sim \sqrt{2}a_p$, $b \sim 2a_p$ and $c \sim \sqrt{2}a_p$, where a_p is the parameter of the perovskite cubic phase.[10] In the orthorhombic structure with *Pnma* space group, Co and Mn ions are randomly distributed at the $6c$ crystallography site. A completely disordered cationic structure should result in changes in structural and magnetic properties compared to the monoclinic ordered phase.

The calculated structural parameters for the cation disordered orthorhombic phase of studied compounds at ambient conditions are: $a = 5.602(3)$ Å, $b = 7.483(3)$ Å, $c = 5.239(2)$ Å for $YCo_{0.5}Mn_{0.5}O_3$ and $a = 5.489(2)$ Å, $b = 7.562(3)$ Å, $c = 5.4381(2)$ Å for $LaCo_{0.5}Mn_{0.5}O_3$. These values are in agreement with the results obtained previously.[10,26] The average crystallite size and microstrain can be estimated by using the Williamson-Hall method based on the $2\theta_{hkl}$ position dependence of peak broadening value β_{hkl} after subtracting the instrumental broadening contribution. The crystalline size of 503(7) nm and the low value of macrostrain of 0.002 (9)% for $LaCo_{0.5}Mn_{0.5}O_3$, and 582(4) nm and $\varepsilon = 0.003(1)\%$ for $YCo_{0.5}Mn_{0.5}O_3$, respectively, confirm the high quality of the synthesized samples.[27]

The temperature dependences of the lattice parameters of $YCo_{0.5}Mn_{0.5}O_3$ and $LaCo_{0.5}Mn_{0.5}O_3$ obtained from X-ray diffraction are shown in Figs. 2(a) and 2(b). It should be noted that the orthorhombic phase with the space group *Pnma* remains down to the lowest temperatures in the experiment. The unit cell volume exhibits strongly anisotropic thermal expansion for both compounds, with the *a*-axis showing the most significant variation. We assumed that the anomaly in the temperature behavior of the lattice parameter is associated with the formation of a FM ordering[26] in the $LaCo_{0.5}Mn_{0.5}O_3$ compound at temperatures below $T < 220$ K. A similar situation is observed for the $YCo_{0.5}Mn_{0.5}O_3$ compound. At temperatures below ~ 76 K, there are clear anomalies in the temperature behavior of *a*, *b* and *c* unit cell parameters. The temperature dependences of the unit cell volume of $YCo_{0.5}Mn_{0.5}O_3$ and $LaCo_{0.5}Mn_{0.5}O_3$ are shown in Fig. 2(c). For temperatures $T > T_C$, the volume thermal expansion coefficients $\alpha_V = (1/V)(dV/dT)$ are $\alpha_V = 1.6(1) \cdot 10^{-5}$ K^{-1} for $YCo_{0.5}Mn_{0.5}O_3$ and $\alpha_V = 2.5(2) \cdot 10^{-5}$ K^{-1} for $LaCo_{0.5}Mn_{0.5}O_3$. At temperatures below the Curie temperature, the volume thermal expansion coefficients change to $\alpha_V = 1.03(1) \cdot 10^{-5}$ K^{-1} for $YCo_{0.5}Mn_{0.5}O_3$ and $\alpha_V = 1.27(1) \cdot 10^{-5}$ K^{-1} for $LaCo_{0.5}Mn_{0.5}O_3$. The changes in thermal expansion coefficients can be explained by the formation of magnetic order in the orthorhombic phase of the studied perovskite materials.[26]

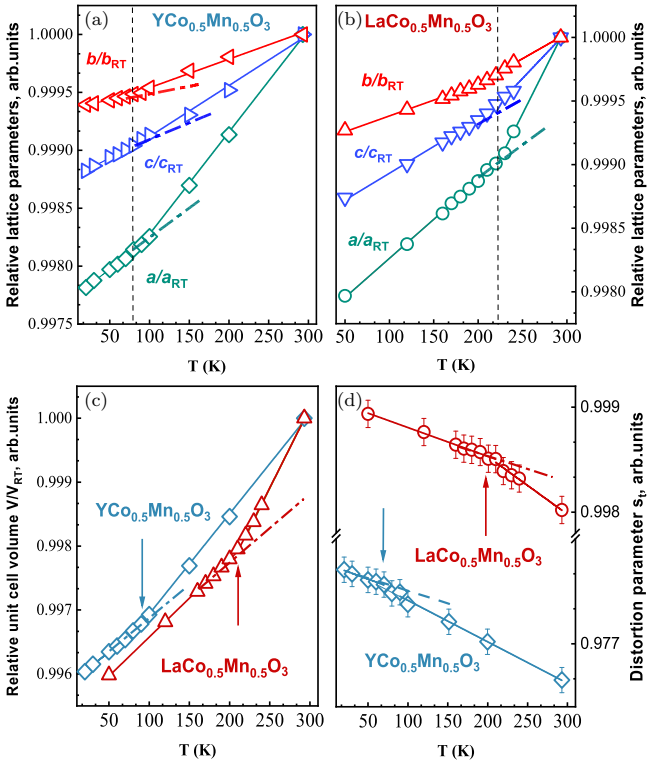

Fig. 2. (Color online) The temperature dependences of lattice parameters normalized to the value of the ones at room temperature for $YCo_{0.5}Mn_{0.5}O_3$ (a) and $LaCo_{0.5}Mn_{0.5}O_3$ (b) and relative volume V/V_{RT} (c) obtained from X-ray diffraction measurements. The dotted lines are approximations of the linear function for regions in the vicinity of critical temperatures. The temperature dependence of distortion parameter s_t (d). The arrows indicate the break points on the temperature dependences, which correspond to magnetic ordering temperatures in the studied compounds.

The uniaxial compression anisotropy can be characterized by a distortion parameter $s_t =$ parameter $s_t = b/\sqrt{2ac}$, where a, b, c are lattice parameters of an orthorhombic structure.[28,29] The s_t parameter is equal to unity for the ideal cubic perovskite cell. The value of s_t decreases from 0.978 to 0.977 for $YCo_{0.5}Mn_{0.5}O_3$ at temperature below $T < T_C \sim 76$ K and from 0.999 to 0.998 for $LaCo_{0.5}Mn_{0.5}O_6$ at temperature below $T < T_C \sim 218$ K (Fig. 2(d)).

The orthorhombic *Pnma* crystal structure contains disordered Mn(Co)O_6 octahedral units.[22] One pair of axial Mn(Co)-O bonds is directed along the b axis, and two pairs of apical bonds lie in the (ac) crystallographic plane. Based on the obtained X-ray diffraction data, the average bond length <Mn(Co)-O> was calculated which mediates magnetic interactions between transition metal ions (Figs. 3(a) and 3(b)). It can be seen that, close to the magnetic phase transition temperature, the anomalies in the behavior of bond lengths are observed in both samples. The Mn(Co)-O-Mn(Co) valence angles are 162.5(5)° at room temperature for the $YCo_{0.5}Mn_{0.5}O_3$,

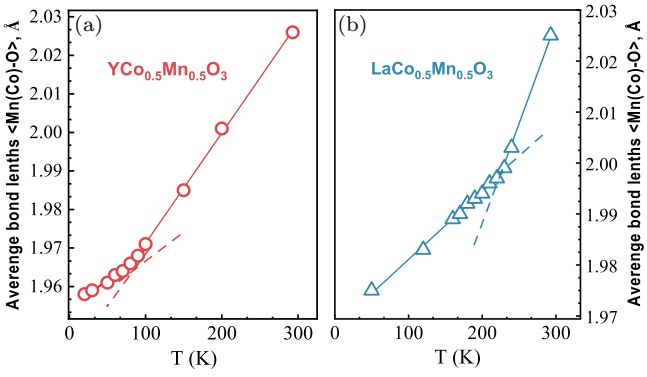

Fig. 3. (Color online) The temperature dependences of average lengths of Mn(Co)-O bond of octahedral coordination in the crystal structure of $YCo_{0.5}Mn_{0.5}O_3$ (a) and $LaCo_{0.5}Mn_{0.5}O_3$ (b). The solid lines represent a linear fir of the experimental data. The dotted line is an approximation of the linear function for regions in the vicinity of critical temperatures.

and 168.3(5)° for the $LaCo_{0.5}Mn_{0.5}O_3$ compound, and they decrease slightly by no more than 0.5°.

3.2. *Neutron diffraction*

Neutron powder diffraction patterns of $YCo_{0.5}Mn_{0.5}O_3$ and $LaCo_{0.5}Mn_{0.5}O_3$ obtained at ambient and low temperatures are shown in Figs. 4(a) and 4(b). At low temperatures down to 15 K, the compounds preserve the orthorhombic crystal structure with *Pnma* space group. It is significant to highlight that, in contrast to X-ray diffraction, neutron diffraction provides a precise approach for directly determining the distribution of Co and Mn across certain crystallographic sites, owing to the substantial disparity in the neutron scattering lengths[30] of Co (2.49 fm) and Mn (−3.73 fm). Analysis of neutron diffraction data for the Co/Mn occupation of the octahedral site indicates that this position is almost half-filled with cobalt and manganese ions. This confirms the model of an orthorhombic crystal structure with disordered cobalt and manganese cations.[31]

Upon cooling, an increase in the intensities of the diffraction peaks (020)/(101) at *d*-spacing $d_{hkl} \approx 2.80$ Å and (121)/(200)/(002) at $d_{hkl} \approx 3.94$ Å was observed, indicating the appearance of long-range magnetic order.[32–34] The intensity of these reflections increases as the temperature decreases. The analysis of the magnetic contribution to neutron diffraction data suggests the parallel arrangement of Mn (Co) spins, oriented along the *b*-axis. The average values of the ordered magnetic moment of Mn(Co) are calculated as $M = 1.9(2)\mu_B$ for $LaCo_{0.5}Mn_{0.5}O_3$ (at $T = 15$ K) and $M \approx 1.4(1)\mu_B$ for $YCo_{0.5}Mn_{0.5}O_3$ compound (at $T = 30$ K). It seems that long-range ferromagnetic order is partially suppressed by structurally disordered occupancy of Co and Mn ions in $YCo_{0.5}Mn_{0.5}O_3$ and $LaCo_{0.5}Mn_{0.5}O_3$.[32–34]

The temperature dependences of the average Mn(Co) magnetic moment are shown in Fig. 4(c). In order to obtain the Curie temperature T_C for the ferromagnetic

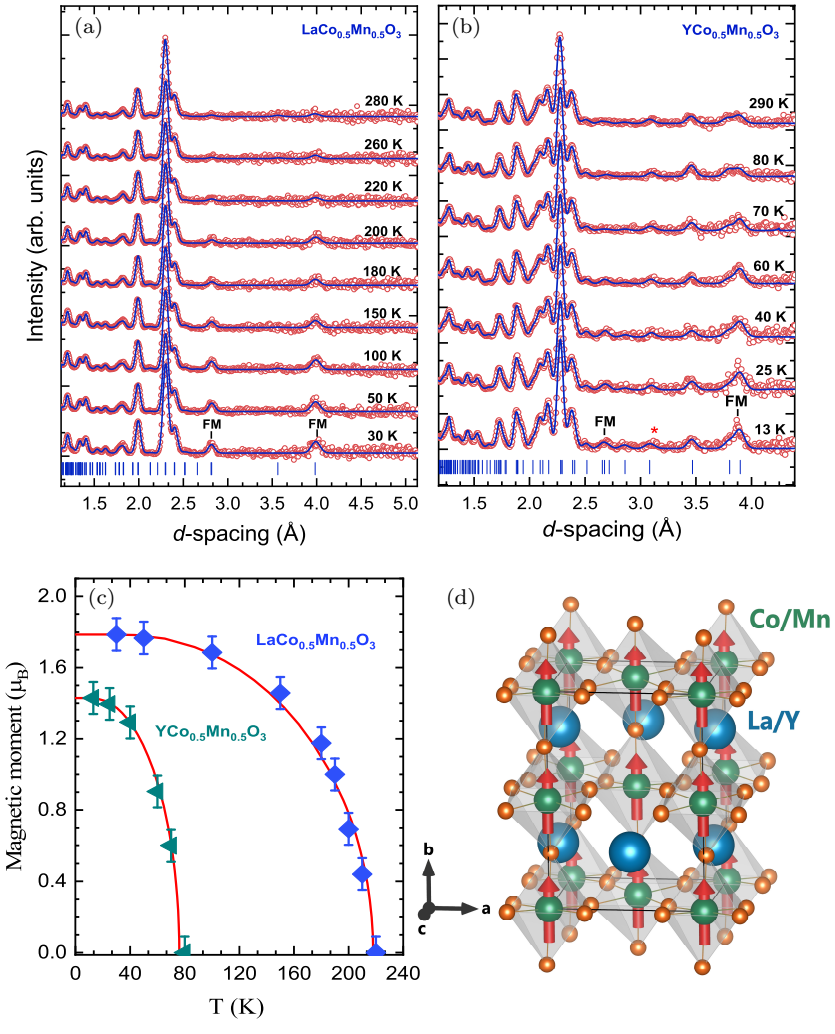

Fig. 4. (Color online) (a) Neutron diffraction patterns of $LaCo_{0.5}Mn_{0.5}O_3$ and $YCo_{0.5}Mn_{0.5}O_3$ measured at low temperatures and refined using the Rietveld method. Experimental points and calculated profiles are shown. Ticks below represent calculated positions of the nuclear peaks of the orthorhombic *Pnma* phase. The peaks with ferromagnetic contribution are denoted by the symbol "FM". (b) Temperature dependences of the average magnetic moment of Mn(Co) ions for the FM phases. The solid lines present a fit of the experimental data using function (1).

phase, the $M(T)$ data was fitted by the function[35]:

$$\frac{M}{M_0} = B_s\left(\frac{3S}{S+1}\frac{M}{M_0}\frac{T_c}{T}\right), \tag{1}$$

where B_S is the Brillouin function, S is the spin of the system ($S = 3/2$) and M_0 is the magnetic moment at $T = 0$. The calculated values of T_C are 76(1) K and 218(1) K for $YCo_{0.5}Mn_{0.5}O_3$ and $LaCo_{0.5}Mn_{0.5}O_3$, respectively.

4. Conclusions

The results of our study show that cation-disordered perovskites $LaCo_{0.5}Mn_{0.5}O_3$ and $YCo_{0.5}Mn_{0.5}O_3$ exhibit an orthorhombic structure with the *Pnma* space group, in comparison to the monoclinic structure, which is typical for cation-ordered double perovskites. This leads to the formation of ferromagnetic ordering in $YCo_{0.5}Mn_{0.5}O_3$ at $T_C = 76(1)$ K and $LaCo_{0.5}Mn_{0.5}O_3$ at $T_C = 218(1)$ K, with comparable low values of ordered magnetic moments. Phase transition from paramagnetic to ferromagnetic phase is accompanied by anomalies in the temperature behavior of the lattice parameters and the distortion coefficient of the octahedral structural units.

Acknowledgements

This work has been supported by the joint grants of the Russian Science Foundation, RSF No:24-42-04002, https://rscf.ru/project/24-42-04002/ and the grant of the Vietnam Academy of Science and Technology, QTRU06.07/24-26.

ORCID

L. H. Khiem https://orcid.org/0000-0001-6869-8976
S. E. Kichanov https://orcid.org/0000-0002-2324-3051
O. N. Lis https://orcid.org/0000-0001-7688-8702
N. T. Nguyen https://orcid.org/0009-0009-1282-8933
E. V. Lukin https://orcid.org/0000-0002-1393-0202
T. N. Vershinina https://orcid.org/0000-0002-7748-5443
D. P. Kozlenko https://orcid.org/0000-0001-9818-9507
N. O. Golosova https://orcid.org/0000-0002-7424-8995
N. Truong-Tho https://orcid.org/0000-0002-1538-1999
N. T. Dang https://orcid.org0000-0003-3480-1888
T. P. Hoang https://orcid.org/0009-0006-3261-3874

References

1. G. A. Smolenskiĭ and I. E. Chupis, *Sov. Phys. Uspekhi* **25**, 475 (1982).
2. T. Kimura *et al.*, *Nature* **426**, 55 (2003).
3. S. Dong and J. M. Liu, *Mod. Phys. Lett. B* **26**, 1230004 (2012).
4. M. M. Vopson, *Crit. Rev. Solid State Mater. Sci.* **40**, 223 (2015).
5. S. A. Wolf *et al.*, *Science* **294**, 1488 (2001).
6. R. Shaheen and J. Bashir, *Solid State Sci.* **12**, 1496 (2010).
7. A. P. Sazonov *et al.*, *Phys. Status Solidi* **244**, 3367 (2007).
8. M. P. Singh *et al.*, *J. Magn. Magn. Mater.* **321**, 1743 (2009).
9. D. C. Kakarla *et al.*, *J. Am. Ceram. Soc.* **97**, 2858 (2014).
10. R. I. Dass and J. B. Goodenough, *Phys. Rev. B* **67**, 14401 (2003).
11. Y. Jia *et al.*, *J. Magn. Magn. Mater.* **481**, 156 (2019).
12. R. C. Sahoo, S. Das and T. K. Nath, *J. Magn. Magn. Mater.* **460**, 409 (2018).
13. T. Jia *et al.*, *J. Appl. Phys.* **117**, 17E119 (2015).

14. H. Chang *et al.*, *J. Alloys Compd.* **690**, 8 (2017).
15. R. P. Madhogaria *et al.*, *J. Magn. Magn. Mater.* **507**, 166821 (2020).
16. R. X. Silva *et al.*, *J. Alloys Compd.* **661**, 541 (2016).
17. R. Das and R. N. P. Choudhary, *Ceram. Int.* **47**, 439 (2021).
18. C. Zhang *et al.*, *J. Electron. Mater.* **43**, 1071 (2014).
19. I. O. Troyanchuk *et al.*, *J. Exp. Theor. Phys.* **99**, 363 (2004).
20. F. N. Sayed *et al.*, *Zeitschrift Für Anorg. Und Allg. Chemie* **640**, 1907 (2014).
21. S. Yáñez-Vilar *et al.*, *J. Alloys Compd.* **485**, 82 (2009).
22. K. D. Truong *et al.*, *Phys. Rev. B* **76**, 132413 (2007).
23. C. L. Bull, D. Gleeson and K. S. Knight, *J. Phys. Condens. Matter* **15**, 4927 (2003).
24. D. P. Kozlenko *et al.*, *Crystallogr. Rep.* **66**, 303 (2021).
25. J. Rodríguez-Carvajal, *Phys. B Condens. Matter* **192**, 55 (1993).
26. P. A. Joy *et al.*, *Mater. Lett.* **46**, 261 (2000).
27. N. T. Dang *et al.*, *J. Electron. Mater.* **46**, 3373 (2017).
28. E. J. Mittemeijer and U. Welzel, *Zeitschrift für Kristallographie* **223**, 552 (2008).
29. D. P. Kozlenko *et al.*, *Phys. Rev. B* **107**, 144426 (2023).
30. J. Dawidowski *et al.*, *Neutron Scatt. – Fundam.* **44**, 471 (2013).
31. M. Mouallem-Bahout *et al.*, *Prog. Solid State Chem.* **35**, 257 (2007).
32. R. P. Madhogaria *et al.*, *Phys. Rev. B* **99**, 104436 (2019).
33. M. T. Vu *et al.*, *J. Alloys Compd.* **681**, 527 (2016).
34. L. O. Troyanchuk *et al.*, *J. Exp. Theor. Phys.* **120**, 97 (2015).
35. T. Maitra and A. Taraphder, *Phys. Rev. B* **68**, 174416 (2003).